Solar Variability and Thermal Inertia in Small CSP Plants

Fernando G. Souza[1], Nicolas Rodio[1], Nelson Y. L. Pabon[1], and Marcia B. H. Mantelli[1]

[1] Federal University of Santa Catarina, Florianópolis (Brazil)

Abstract

Concentrated Solar Power (CSP) plants convert solar energy into thermal energy through collector mirrors that concentrate solar radiation onto a working fluid, which transfers the heat to a power cycle. These plants are modeled considering two main subsystems: the solar field, responsible for capturing and transferring thermal energy, and the power cycle, responsible for converting this energy into electricity. This study analyzes solar variability and thermal inertia in a small-scale CSP plant operating with and without a thermal energy storage (TES) system under irradiance conditions typical of Florianópolis and Brasília. The solar field employs parabolic collectors and Thermisk as the heat transfer fluid, while the thermal energy storage system uses Syltherm™ XLT in sensible heat operation. The implemented power cycle was a simple Organic Rankine Cycle (ORC) operating with the R152a refrigerant. Summer and winter conditions were simulated based on direct normal irradiance (DNI) data obtained from the SONDA solar measurement network. The results indicate that the presence of TES increases the stability and continuity of generation, reducing the plant's sensitivity to DNI fluctuations. Additionally, thermal storage was found to contribute to higher operational reliability and better utilization of solar resource in small-scale CSP plants.

Keywords: Concentrated Solar Power, Thermal Energy Storage, Organic Rankine Cycle, Solar Variability, Thermal Inertia

1. Introduction

Heliothermal plants or CSP plants, are electricity generation systems based on the conversion of solar energy into thermal energy and, subsequently, into electrical energy. These plants typically operate with two interconnected circuits (Fig. 1): the solar field, responsible for concentrating solar radiation and heating a heat transfer fluid, and the power conversion cycle, in which thermal energy is converted into mechanical energy and then into electricity, using a Rankine cycle.

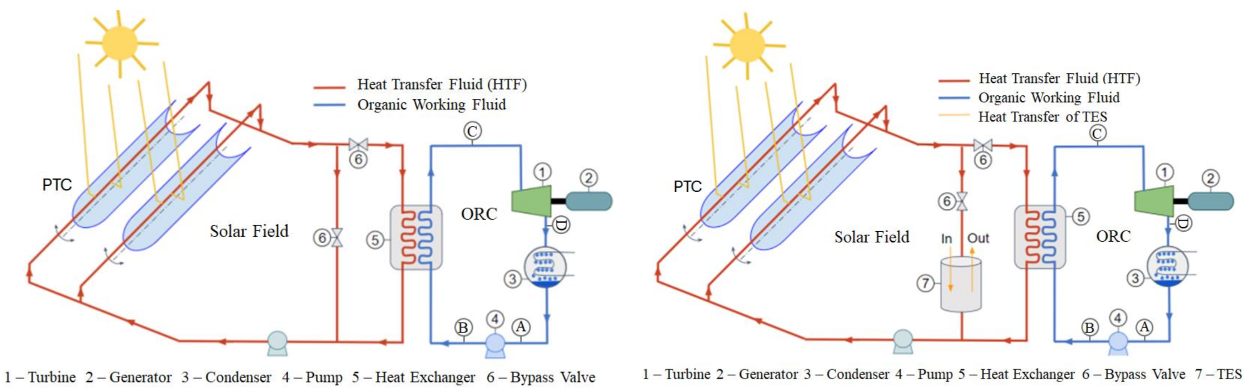

(a) Small-scale CSP without TES. (b) Small-scale CSP with TES.

Figure 1 – Schematic representation of the two studied CSP plant configurations.

Depending on the design, CSP plants can operate without thermal energy storage (TES) (Fig. 1a) or with TES (Fig. 1b), which allows energy to be stored in reservoirs for later conversion into electricity, ensuring dispatchability even at night or under unfavorable weather conditions (Heller, 2017).

10.18086/swc.2025.01.23 Available at http://proceedings.ises.org

The main limitation of CSP plants is associated with climatic variability, which affects the availability of solar radiation and, consequently, system performance. This variability occurs on different temporal scales – daily, between consecutive days, or seasonally – and can be assessed using parameters such as the Cloudless Percentage Days (CPD), which indicates the frequency of clear-sky days (Rocha et al., 2022), and Direct Normal Irradiance (DNI), which represents the solar flux incident on a surface normal to the sun's rays (Heller, 2017). Both indicators are location-specific and determine the technical and economic feasibility of a CSP plant.

In small-scale plants, the influence of solar variability is even more significant. Therefore, understanding the system's thermal response to irradiance fluctuations is essential to estimate its performance and reliability. Accordingly, this study aims to evaluate the thermal inertia of a small-scale CSP plant, comparing two configurations (with and without TES) under irradiance conditions representative of Florianópolis and Brasília on typical summer and winter days. These locations were selected due to their contrasting solar radiation levels within the Brazilian context.

2. Variability of the Brazilian Solar Resource

The operation of CSP plants is influenced by fluctuations in solar irradiance, which directly affect the energy balance of the solar field and the system's thermal response. To analyze the thermal inertia of the plant, it is necessary to understand how these fluctuations occur and how they can be quantified. Several methodologies have been proposed in the literature to measure the degree of variability of the solar resource through specific indices, which allow for the assessment of generation stability and predictability over time.

The characterization of these fluctuations, which correspond to the variability of the solar resource, aims to describe changes in the irradiance incident on the Earth's surface at a given location and time interval. According to Kariuki and Sato (2018) and Davy and Troccoli (2012), long-term fluctuations (annual and decadal) are associated with astronomical and climatic factors, such as the solar cycle, the Earth's orbital eccentricity, and global atmospheric patterns. Short-term variations (hourly or sub-hourly), on the other hand, mainly arise from transient atmospheric phenomena, such as cloud movements, precipitation, and the presence of aerosols.

Rocha et al. (2021) proposed a methodology to assess the variability of global horizontal irradiance at three stations of the SONDA network (INPE), classifying days into four sky conditions: clear (CS), cloudy (CL), scattered cloudy (SC), and high variability (HV). Two indicators were used for this purpose: (i) the variability index (VI), defined as the ratio between the length of the measured irradiance curve and the clear-sky curve (Stein et al., 2012), see Fig. 2a, and (ii) the relative ramps index (RR), adapted from Zhu et al. (2019) (Fig. 2b). Cluster analysis between the clearness index and VI revealed typical "arrowhead"-shaped patterns for the three SONDA stations, without a clear predominance of any sky type. The results confirmed the feasibility of using these indices and statistical tools to characterize solar measurement stations, suggesting that the methodology could be extended to other SONDA stations and that satellite images could be employed to expand the study points across Brazil.

Subsequently, Rocha et al. (2022) introduced the CPD index, which combines variability and availability of the solar resource to assess the quality of Brazil's solar resource. Using nine years of data from the SONDA network and images from the GOES-13 satellite, a strong correlation was observed between ground-based and satellite-based approaches. The annual CPD mapping (Fig. 3a) revealed a higher percentage of cloudless days along the Brazilian "solar belt," a spatial pattern similar to the solar potential map for CSP generation by Pereira et al. (2017) (Fig. 3b).

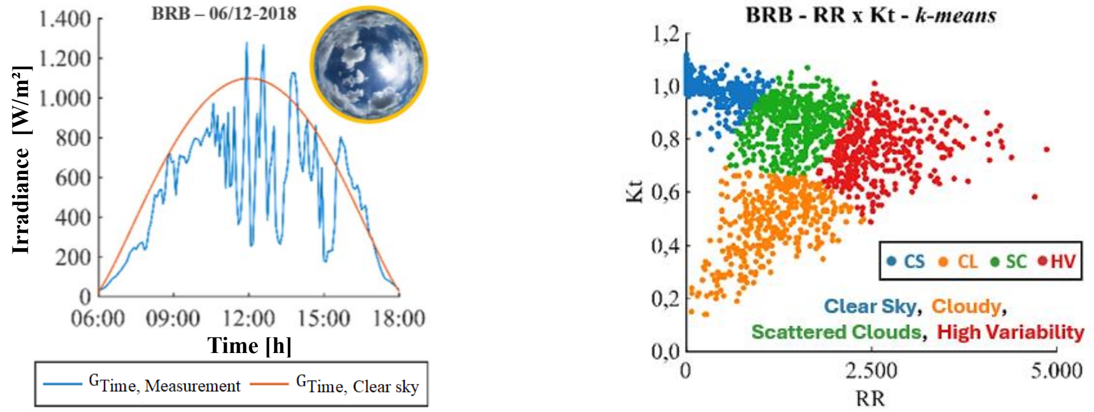

(a) Measured hourly irradiance and under clear-sky conditions. (b) Classification of sky types obtained using the k-means method.

Figura 2. Measured irradiance and sky type classification for the SONDA station in Brasília/DF. Source: Adapted from Rocha et al. (2021).

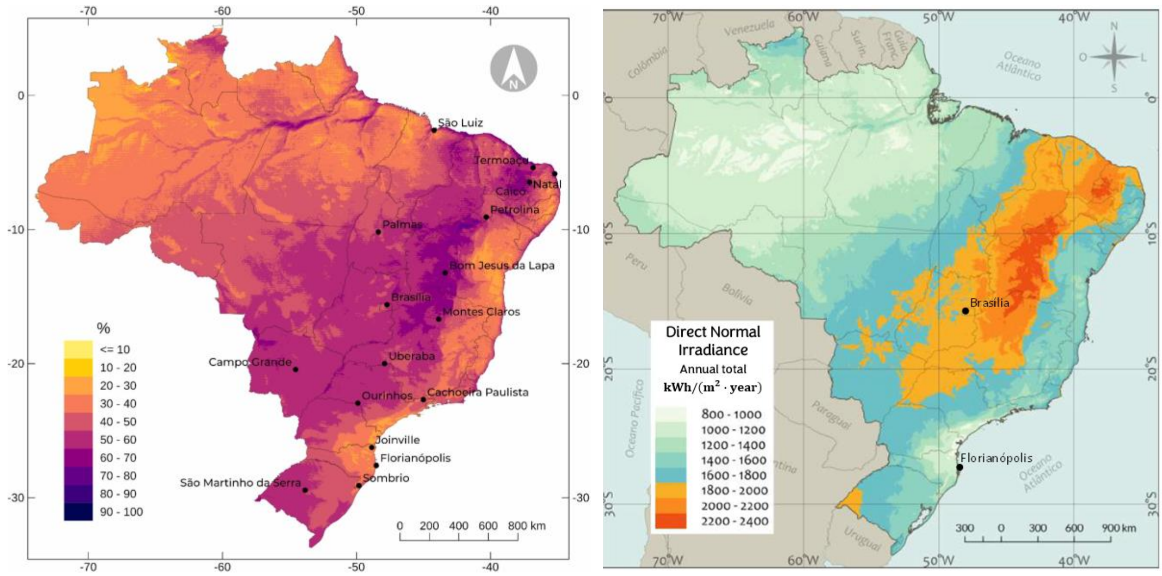

(a) Annual CPD index, estimated from satellite data. Source: Rocha et al. (2022).

(b) Annual total of Direct Normal Irradiance (DNI). Source: Pereira et al. (2017).

Figura 3. Maps of the CPD index and Direct Normal Irradiance (DNI) in Brazil.

The comparison between the CPD and DNI maps shows a general correspondence between regions with the highest solar potential and those with high resource stability. However, some areas — such as northern Roraima, the Piauí–Maranhão border, northern Mato Grosso do Sul, the border with São Paulo, and the far southwest of Rio Grande do Sul — exhibit high CPD values (above 60) despite moderate DNI levels. This discrepancy may be associated with local atmospheric and topographic conditions that reduce hourly variability and favor consistent solar generation throughout the day, an aspect relevant for analyzing the thermal inertia of CSP systems.

As indicated by de Souza et al. (2024), when comparing Brazil's solar potential with that of Germany, it is observed that, although the climatic and geographic contexts are distinct, Brazil exhibits average irradiance levels up to twice as high. Regions such as the semi-arid Northeast and the Central-West stand out for their high solar radiation availability and low intra- and interannual variability, creating a highly favorable scenario for CSP generation. In contrast, Germany, even with a more limited and variable resource, has successfully expanded solar energy through public policies and robust technological investments — demonstrating that the exploitation of Brazil's potential also depends on an adequate institutional and technological framework.

3. Methodology for Analyzing Thermal Inertia in Small CSP Plants

For the modeling of the CSP plant, a description of the circuits that compose the studied plant is presented:

3.1 Solar Field

In this study, the solar field was modeled considering two distinct configurations, depending on the presence or absence of a thermal energy storage system.

In the configuration without storage, the solar field consists of a solar collector, a pump, a bypass valve, and a heat exchanger (HE). In this arrangement, the collector concentrates solar radiation onto a receiver (the highest-temperature region of the circuit, located at the focus of the concentrators), heating the working fluid circulating within. This fluid is recirculated through the bypass valve until it reaches a sufficiently high temperature to transfer energy to the secondary circuit via the HE.

In the configuration with energy storage, a thermal tank is added after the bypass valve. This reservoir allows the accumulation of thermal energy through sensible heat storage, providing greater operational flexibility to the plant. In this configuration, initial operation occurs when the working fluid reaches the temperature required for heat exchange with the secondary circuit. At this stage, the tank acts as an intermediate storage medium, accumulating thermal energy before the fluid is directed to the heat exchanger.

The working fluid of the solar field generally operates in a single-phase liquid state. It must be designed or selected to withstand the high temperatures reached in the receivers while exhibiting low degradation over its service life. Since CSP plants employ the principle of solar concentration to raise the temperature of the primary fluid (which transfers energy to the secondary circuit via the HE), any variation in solar irradiance directly impacts the behavior of the Rankine cycle (Pabon et al., 2024). In this study, the thermal fluid used in the solar field circuit was Termisk.

3.2 Rankine Cycle

For the present analysis, a simple ORC was considered (Fig. 1). The circuit consists of four elements: (a) a pump that compresses the fluid (points A→B); (b) a heat exchanger that adds heat at constant pressure (points B→C); (c) a turbine that converts mechanical energy into electricity (points C→D); and (d) a condenser that rejects heat at constant pressure (points D→A).

For the Rankine cycle, R152a was used as the working fluid. The fluid enters the pump as a saturated liquid and exits pressurized, reaching a subcooled region up to the operating pressure of the heat exchanger. In the heat exchanger, the compressed liquid is converted into vapor due to the addition of heat from the CSP plant's solar field. The high-energy vapor expands in the turbine, converting the fluid's thermal energy into rotational kinetic energy. As the turbine and the electric generator share the same shaft, this rotational motion drives electricity generation. Next, the fluid enters the condenser as saturated vapor and, through heat rejection to the environment, is converted into saturated liquid. This configuration completes the phase-change cycle of the working fluid, making it available to be compressed again by the pump.

The pump and the boiler add work and energy to the system, while the turbine and the condenser extract work and energy from the system, respectively. The difference between the work extracted by the turbine and the work added by the pump results in the net work for electricity generation, while the ratio of net work to the heat added in the boiler represents the cycle's thermal efficiency.

3.3 CSP Plant Modeling

The energy potential of a CSP plant depends on the local DNI and is influenced by factors such as rainfall and cloud cover. Plant design must consider the collector field area (A), ambient temperature

(T_{amb}), and concentration factor (CF), which determine the heat transfer rate to the primary fluid. Since not all incident solar energy is captured, collector efficiency ($\eta_{Collector}$) is used to estimate the useful thermal flux. In this study, a Parabolic Trough Collector (PTC) was used, converting 45% of the incident solar energy into thermal energy.

The analysis used DNI data from two Brazilian meteorological stations, Florianópolis (FLN) and Brasília (BRB), chosen for their contrasting solar intermittency, climatic conditions, and observed CPD values. Two typical days of the year 2014 were selected to capture seasonal variations: one in summer (January) and one in winter (July). In Florianópolis, summer presented low solar intermittency with DNI values near 1000 W/m², while in winter the maximum reached about 800 W/m², despite generally high CPD throughout the year. In Brasília, DNI often exceeds 1000 W/m²; however, summer rains reduce direct radiation availability, whereas the dry and stable winter climate favors high CPD values and greater solar energy capture.

Thus, for modeling the solar field, two distinct approaches were adopted: one for the field without a thermal energy storage (TES) system and another with TES.

- ✓ **Solar Field without TES**

In this study, it was assumed that the solar field begins operation when the DNI exceeds 30 W/m². If, during operation, the DNI falls below this threshold, the plant's operation is temporarily interrupted, representing solar intermittency caused by passing clouds.

After the start of operation, the thermal power incident on the receiver is calculated based on the solar radiation data and the geometric and optical properties of the PTC, as follows:

$$\dot{Q}_{solar} = CF \cdot A \cdot \eta_{Collector} \cdot DNI[i] \quad \text{(eq.1)}$$

The performance of the solar field is affected by heat losses to the environment, mainly due to convection and radiation.

Convective losses are estimated according to the correlation proposed by Ferreira et al. (2018):

$$\dot{Q}_{convection} = L \cdot (a_0 \cdot \Delta T + a_1 \cdot \Delta T^2) \quad \text{(eq.2)}$$

where the temperature difference (ΔT) is given by:

$$\Delta T = \frac{T_{out} + T_{in}}{2} - T_{amb} \quad \text{(eq.3)}$$

Here, T_{out} and T_{in} are the outlet and inlet temperatures of the solar collector, respectively; L is the collector length; $a_0 = 0.67$ W/(m·K) and $a_1 = 0.00256$ W/(m·K²) are thermal loss coefficients. The radiative losses are determined by the following expression:

$$\dot{Q}_{radiation} = \sigma \cdot A_{receiver} \cdot \left(\Delta T^4 - T_{amb}^4\right) \quad \text{(eq.4)}$$

where $\sigma = 5.67 \cdot 10^{-8} W/m^2K^4$ is the Stefan–Boltzmann constant, and $A_{receiver}$ is the receiver area. The total heat loss ($\dot{Q}_{losses}$) is obtained by summing Equations (2) and (4), and the outlet temperature of the thermal fluid in the PTC (T_{out}) is determined from the energy balance:

$$T_{out} = T_{in} + \frac{\dot{Q}_{solar} - \dot{Q}_{losses}}{\dot{m}_{solar} \cdot c_{p_{Termisk}}} \quad \text{(eq.5)}$$

An iteration is necessary, where in the first guess, it is assumed that $T_{in} = T_{amb}$. In subsequent simulation steps, T_{in} is updated dynamically at each time interval, util convergence.

- ✓ **Solar Field with TES**

For the TES system, a single-tank thermally stratified model was considered. This configuration was adopted due to its simplicity and suitability for small-scale CSP plants, compared to systems with separate hot and cold fluid tanks (Wendel et al., 2013).

Thermal stratification naturally occurs due to density differences between fluid layers: hotter regions tend to remain at the top of the tank, while cooler regions settle at the bottom. Thus, the cold fluid feeding the solar field is drawn from the lower section of the tank, and the heated fluid is extracted from the upper section.

In the adopted model, two non-mixing fluid volumes are considered, representing the hot and cold regions. The mass flow rate in both circuits remains constant throughout the simulation, and the fluid coming from the solar field enters the storage tank at a fixed flow rate. Figure 1b illustrates the schematic of the solar field coupled to the TES system.

In this configuration, a bypass valve controls the flow direction of the Termisk thermal oil at the outlet of the PTC toward the TES. At this point, the heat transfer fluid (HTF) may either release or absorb additional thermal energy from the TES, depending on the system's operating state. Alternatively, the HTF can return to the PTC to absorb more solar radiation and increase its temperature or, if it already contains sufficient energy, transfer heat to the ORC for power generation.

For the thermal storage medium, Syltherm™ XLT was used, operating under sensible heat storage (without phase change) within a temperature range of 280 K to 550 K, compatible with typical operating conditions of small-scale CSP systems.

The adopted storage tank has a height of 1.6 m, diameter of 0.6 m, and contains approximately 300 kg of Syltherm™ XLT. The model used is based on Araújo (2017), which describes the TES energy balance considering thermal losses by conduction through the tank walls, convection to the ambient air, and radiation. In this work, an average TES efficiency of 0.85 was adopted, representing the global estimate of system heat losses. The CSP plant model with TES maintains the same operating conditions as the plant without TES, that is, operation during the day and during periods of solar intermittency. The main difference occurs during start-up, when the thermal model considers an operation temperature range between 510 K and 520 K. At this stage, the heat from the solar field is directed exclusively to the TES tank until it reaches the required operating temperature.

This temperature range was chosen because the solar field provides sufficient energy to start the ORC cycle without the need for additional energy to charge the TES. During the simulation, it is verified whether the TES temperature (T_{TES}) exceeds 520 K.

At the beginning of the day, the TES tank is at ambient temperature and therefore not within the operating range. In this case, the model checks whether the TES temperature is higher than the outlet temperature of the parabolic collector ($T_{TES} \geq T_{out}$). If not, the HTF directs the solar energy to the TES. The thermal exchange between the solar field and the TES is modeled as a HE — the same approach used for the interface between the solar field and the ORC.

The maximum heat transfer rate is given by the following equation:

$$C_{min} = \dot{m}_{solar} \cdot c_{p,Termisk} \quad \text{(eq.6)}$$

as the thermal oil of the solar field has the lowest thermal capacity among the two systems, it follows that:

$$\dot{Q}_{TES} = \eta_{TES} \cdot C_{min} \cdot (T_{out} - T_{TES}) \quad \text{(eq.7)}$$

Considering the maximum possible heat transfer, the TES temperature can be calculated as:

$$T_{TES} = T_{out} - \frac{\dot{Q}_{TES}}{\dot{m}_{Syltherm} \cdot c_{p_{Syltherm}}} \quad \text{(eq.8)}$$

where $\dot{m}_{Syltherm}$ and $c_{p_{Syltherm}}$ are, respectively, the mass flow rate and specific heat of the fluids. The thermal oil circulates through the storage tank, raising the TES temperature (T_{TES}) and also affecting the PTC outlet temperature (T_{out}). The new inlet temperature of the fluid into the PTC (T_{in}) is determined by:

$$T_{in} = T_{out} - \frac{\dot{Q}_{TES}}{\dot{m}_{solar}\, c_{p,Termisk}} \quad \text{(eq.9)}$$

After leaving the tank, the oil returns to the collector, updating the system temperatures in an iterative cycle until a new condition is met. During periods of solar intermittency or after energy transfer to the ORC, the PTC outlet temperature may drop below that of the TES. In this case, if the HTF does not have enough energy to start the ORC, the TES releases stored heat to the thermal oil, raising T_{out} and reducing the total stored energy. The thermal storage capacity of the TES is given by:

$$\Delta Q = \rho\, c_p\, V\, \Delta T \quad \text{(eq.10)}$$

Thus, the stored energy depends directly on the tank volume and the thermophysical properties and (ρ e c_p) of the material. When the TES thermal fluid reaches temperatures above 520 K and the actual enthalpy ($h_{3,real}$) exceeds that required for the operating point (h_3), the HTF has sufficient energy to drive the ORC. Otherwise, the system returns to a condition in which the TES transfers heat to the fluid until the required energy is reached. If the TES still does not provide enough heat, the thermal oil recirculates through the parabolic collector, raising T_{out} again, provided that the DNI is above 30 W/m².

During periods when the TES is not in operation, the storage tank loses heat to the environment via radiation.

For the power cycle, the present model considers that, of the total energy absorbed by the primary circuit, a portion is transferred to the secondary circuit through the heat exchanger, while another portion is lost to the environment.

To model the energy conversion cycle (secondary circuit), the thermodynamic analysis methodology of an ORC was used, taking into account the operational characteristics of each component. For the power generation cycle simulation, the following assumptions were made:

Assumptions for the ORC. The parameters and boundary conditions of a Rankine cycle were established as follows:

- **Point 1:** Saturated liquid with zero quality and a temperature of 25°C;
- **Point 2:** Pump outlet pressure ranging from 2 to 4.3 MPa;
- **Point 3:** Superheated fluid with pressure ranging from 2 to 4.3 MPa;
- **Point 4:** Turbine expansion, pressure equal to that at point 1.

The ORC performance is limited by the plant component characteristics, climatic variability, and the thermophysical properties of the fluids evaluated under the established conditions. For each component of the cycle, the following considerations were adopted:

- ✓ ***Heat Exchanger:***

In the ORC, the heat exchanger is modeled as a counterflow device, where the hot fluid is considered incompressible, and the working fluid may undergo a phase change along the equipment.
The amount of energy available from the heat exchanger for the ORC can be obtained from the enthalpy variation between the inlet and outlet of the device, and is given by:

$$Q_{HE} = \dot{m}_{ORC} \cdot (h_C - h_B) \quad \text{(eq.11)}$$

where $\dot{m}_{ORC}$ represents the mass flow rate of the organic fluid in the energy conversion cycle (kg/s), while (h_B) and (h_C) are the inlet and outlet enthalpies of the boiler, respectively (J/kg).

✓ ***Pump:***

The pump model considers an isentropic device, in which there is no thermal energy loss to the environment and the mass flow rate is constant. The work produced by the pump is given by:

$$W_{Pump} = \dot{m}_{ORC} \cdot (h_B - h_A) \quad \text{(eq.12)}$$

the term (h_A) refers to the enthalpy for the saturated liquid condition at a temperature of 25°C, that is, ($h_A = h(T = 25°C; x = 0)$), given in J/kg.

✓ ***Turbine:***

The turbine model considers an isentropic and adiabatic device. In addition, a turbine with variable geometry (Variable Geometry Turbine, VGT) was selected, which allows the variation of the working pressure by changing the blade angles. The turbine work can be determined from the expansion of the working fluid, given by:

$$W_{Turb.} = \dot{m}_{ORC} \cdot (h_D - h_C) \quad \text{(eq.13)}$$

the term (h_D) refers to the enthalpy for the saturated vapor condition, with units of J/kg.

✓ ***Condenser:***

The modeling of the condenser follows the same assumptions as for the heat exchanger, considering the absence of pressure loss and homogeneous flow. The formulation for the condenser is given by:

$$Q_{Cond} = \dot{m}_{ORC} \cdot (h_A - h_D) \quad \text{(eq.14)}$$

Furthermore, for the condenser, it was assumed that it is connected to a cold source without restrictions on heat supply and mass flow rate. As mentioned previously, the net work of the cycle corresponds to the electrical generation of the CSP plant, determined by:

$$W_{NW.} = W_{Turb.} - W_{Pump} \quad \text{(eq.15)}$$

4. Results and Discussion

To evaluate the CSP plant's operation with and without TES, a Python code simulated two typical days of 2014 — one in summer and one in winter — for Florianópolis (FLN) and Brasília (BRB) using DNI data from the SONDA project. Each component was analyzed by Rodio (2024) for both locations and configurations; however, only the results for Brasília on a typical summer day are detailed. Figure 4 presents the DNI and output variables of each component for both configurations, enabling a direct comparison of the impact of thermal energy storage.

In Fig. 4, the TES enhances the production and stability of the ORC turbine's net work compared to the configuration without TES. The plant without TES shows a behavior that is more sensitive to variations in DNI. The recirculation system allows this setup to quickly reach high temperatures; however, an abrupt drop in DNI caused by short-term solar variability, such as passing clouds, leads to a decrease in temperatures at nearly the same rate as the DNI reduction.

In contrast, the system with TES behaves differently, showing a gradual increase in temperature. This occurs because the thermal energy concentrated by the collector is transferred to the TES. Once the operating temperature is reached, the TES helps make the solar field less sensitive to sudden fluctuations in DNI. The slight decline in temperature after the end of solar irradiation is due to heat losses to the environment.

Analyzing the inlet temperatures of the ORC components for both configurations, it is observed that, except for the turbine inlet, the other temperatures are practically similar. This behavior is explained by the implemented ORC circuit, in which the pressure increase in the pump has a minimal effect on the temperature between the pump inlet and the boiler inlet, since R152a remains in a subcooled liquid state, preventing significant temperature rises. The condenser inlet temperature corresponds to the condition after the turbine performs isentropic expansion until the outlet vapor reaches the saturated vapor state. As condensation occurs isobarically, the inlet temperatures of both the condenser and the pump are similar.

The most sensitive variable to solar irradiation is the turbine inlet temperature. For the CSP without storage, continuous oscillations are observed, directly affecting the net work produced by the ORC. In the configuration with TES, the turbine inlet shows a delay of approximately 160 minutes, followed by a significant reduction in oscillations, indicating that the stored energy compensates for solar variability and enables the turbine to operate in a more stable and efficient manner. The TES analysis indicates that the delay observed in the PTC and turbine inlet temperatures (T3) corresponds to the time required for the storage tank to accumulate sufficient energy to enable ORC operation.

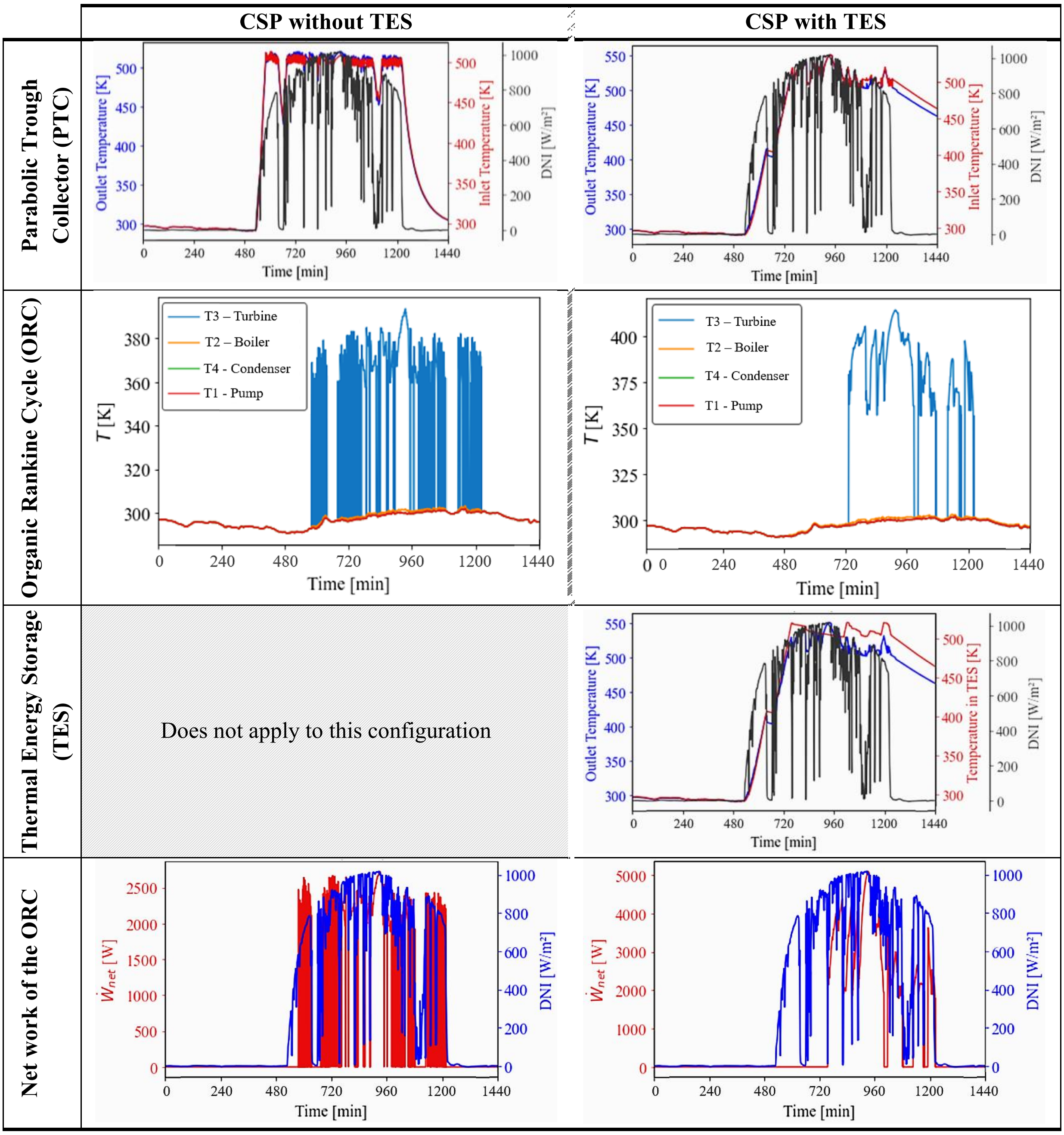

Figura 4. Simulation results of a CSP plant, with and without TES, for a summer day in Brasília/DF.

These results show that small-scale ORC plants without thermal storage are highly susceptible to the solar variability of the installation site. The implementation of TES mitigates these fluctuations, promoting greater stability and energy production. Proper sizing of the solar collector area and TES volume is therefore a determining factor to ensure autonomy and efficiency in the power generation of ORC-based plants.

Figures 5 and 6 show the net work output of the ORC for both CSP configurations, considering DNI values for typical summer and winter days. The data used correspond to the solarimetric stations of the SONDA network in the cities of Florianópolis and Brasília, respectively.

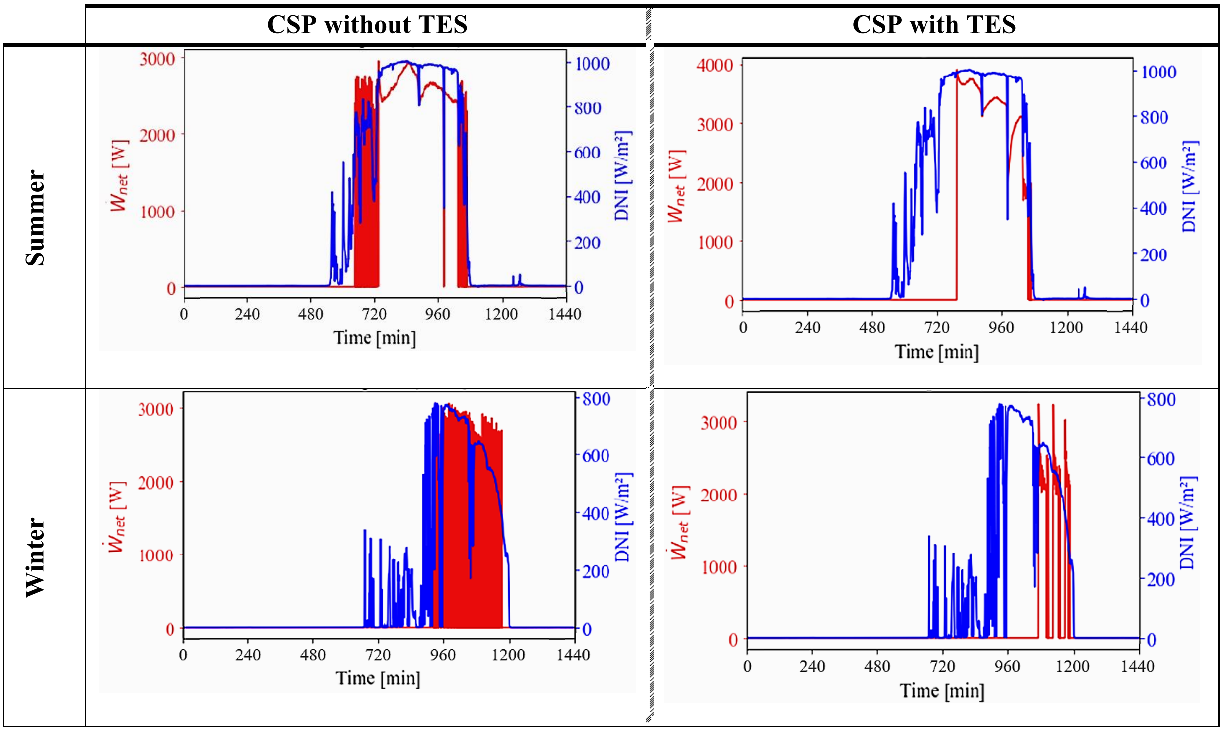

Figure 5. Net work output of the ORC turbine located in the city of Florianópolis for two days in different climatic seasons.

In the analyzed cases for the city of Florianópolis (Fig. 5), it is observed that, according to the DNI profile, both days showed significant cloud cover, affecting at least half of the solar hours. The summer day, however, presented more favorable irradiance conditions compared to winter. Since the performance of CSP plants strongly depends on direct solar irradiance, the thermal behavior and net work production were more stable and efficient during summer. The thermal energy storage (TES) system contributed to this stability by smoothing fluctuations in power generation. In winter, however, its influence was less noticeable, as the high cloudiness during the morning hours prevented the accumulation of sufficient thermal energy for continuous system operation.

For the city of Brasília (Fig. 6), the results show an opposite condition: the summer day exhibited significant cloudiness, while the winter day was characterized by clear skies. In summer, as previously discussed, the use of TES was crucial to stabilize the net power output of the ORC cycle. In winter, the configuration without thermal storage showed more pronounced fluctuations in generated power, as the turbine operated under partial loads, responding directly to DNI oscillations. Conversely, the system with TES presented a delay in the start of operation, but once the steady-state temperature was reached, it maintained continuous and stable operation throughout the period.

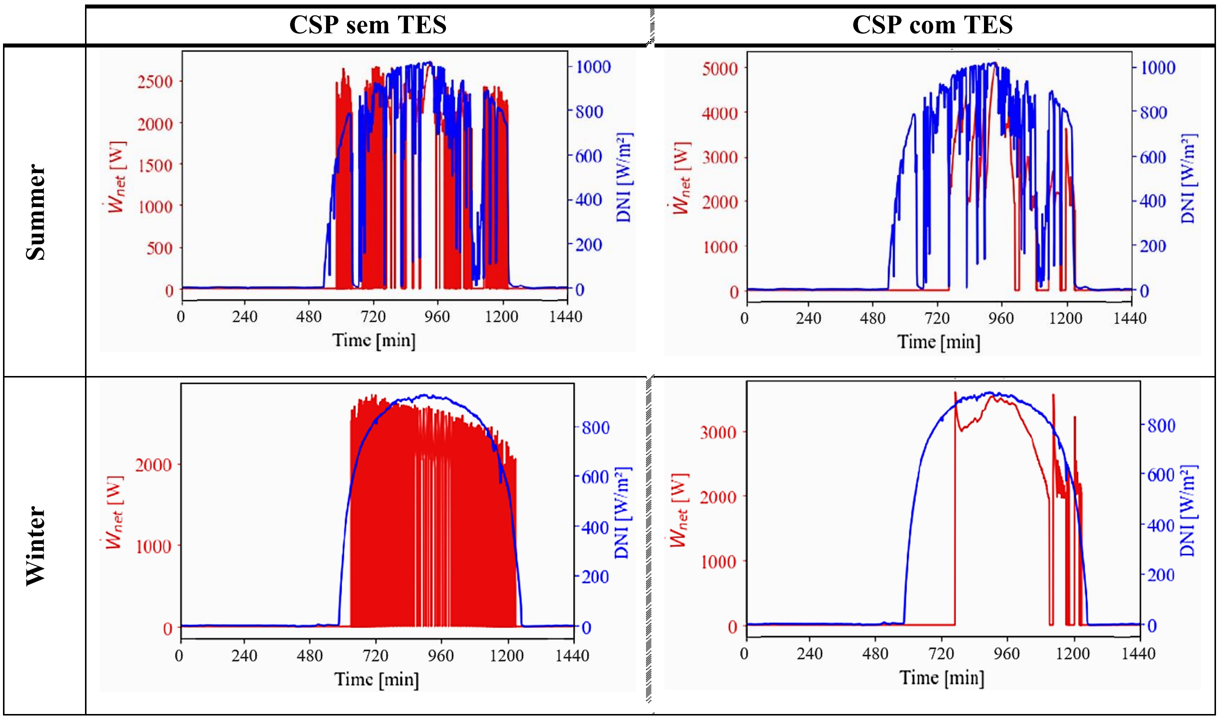

Figure 6. Net work output of the ORC located in the city of Brasília for two days in different climatic seasons.

When comparing the two locations based on the solar variability and annual average DNI maps (Fig. 3), it is confirmed that Brasília has a higher solar potential than Florianópolis. Therefore, the implementation and operation of CSP plants would be more feasible in the federal capital, especially if the project includes higher-capacity thermal storage systems and an expanded solar field. This configuration would enable energy storage during periods of peak irradiance and allow continuous operation of the system even under solar intermittency or reduced DNI at the end of the day.

5. Conclusions

In this study, the performance of a small-scale CSP plant was evaluated under different solar irradiance conditions, considering two configurations — with and without thermal TES — and two Brazilian locations with contrasting radiation profiles: Florianópolis and Brasília. The analyses were carried out for typical summer and winter days to investigate the effects of solar variability and thermal inertia on the dynamic behavior of the system.

The results highlighted the strong influence of solar variability on the plant's thermal and electrical performance. Simulations demonstrated that the DNI profile is the main factor responsible for temperature fluctuations in the solar field and, consequently, for variations in the net power output of the ORC cycle.

The comparison between the analyzed configurations emphasized the importance of the thermal storage system in mitigating these fluctuations. While the plant without TES exhibited highly sensitive behavior to solar variability — with continuous oscillations in turbine inlet temperature and net work output — the inclusion of TES provided greater operational stability and improved solar energy utilization efficiency, especially during periods of high irradiance.

In Florianópolis, high cloudiness significantly reduced the generation potential, particularly in winter, when the TES had limited influence due to insufficient stored energy. Conversely, Brasília presented higher solar potential, resulting in better overall plant performance. Even on days with variability, the system with TES maintained more regular and continuous operation after the initial thermal charging period.

Therefore, thermal energy storage plays a fundamental role in the performance of small-scale CSP plants, as it smooths the system's response to solar variability. Proper sizing of the collector area and TES volume is crucial to ensure operational stability, autonomy, and efficiency in converting solar energy into electricity, especially in regions with high levels of direct irradiance intermittency.

Acknowledgments

The authors would like to thank the Fund for Financing Studies of Projects and Programs (FINEP), Brazilian National Council for Scientific and Technological Development (CNPq), and the Federal University of Santa Catarina (UFSC) for their support.

References

Araújo, A.K.A., 2017. *Transient modeling of thermal storage in CSP systems*. Master's thesis, Brazil.

Davy, R.J., Troccoli, A., 2012. Interannual variability of solar energy generation in Australia. Solar Energy 86(12), 3554–3560.

Ferreira, W. M. 2018. Modelagem termodinâmica de uma planta fresnel com geração direta de vapor e armazenamento de energia térmica.

Heller, P., 2017. The performance of concentrated solar power (CSP) systems: analysis, measurement and assessment. Woodhead Publishing.

Kariuki, B.W., Sato, T., 2018. Interannual and spatial variability of solar radiation energy potential in Kenya using Meteosat satellite. Renewable Energy 116, 88–96.

Pabon, N.Y.L., Souza, F.G., Gatti, G.M., Mantelli, M.B.H., 2024. Análise teórica de uma planta heliotérmica de pequena escala operando com ciclo Rankine Orgânico. In: Proceedings of the X Congresso Brasileiro de Energia Solar, Natal, Brasil.

Pereira, E., Martins, F., Gonçalves, A., Costa, R., Lima, F., Rüther, R., Abreu, S., Tiepolo, G., Pereira, S., Souza, J., 2017. Atlas Brasileiro de Energia Solar, 2nd ed. INPE, São José dos Campos, 80 p.

Rocha, V.R., Rodrigues Gonçalves, A., Santos Costa, R., Bueno Pereira, E., Ramos Martins, F., Onofre Inácio, C., Almeida Fontenele, L.F., Fernandes Ferreira, P.H., 2021. Avaliação da variabilidade do recurso solar em território brasileiro. Revista Brasileira de Energia Solar 12(2), 113–120.

Rocha, V.R., Costa, R.S., Martins, F.R., Gonçalves, A.R., Pereira, E.B., 2022. Variability index of solar resource based on data from surface and satellite. Renewable Energy 201, 354–378.

Rodio, N. 2024. *Impact of solar intermittency on a small-scale concentrated solar power plant in Brazil.* Master's thesis, Brazil.

Souza, F.G., Pabón, N.Y.L., Rodio, N., Krambeck, L., Costa, R.S., Gonçalves, A.R., Mantelli, M.B.H., 2024. Uso da energia termossolar no Brasil: panorama atual e potencial de desenvolvimento. In: Proceedings of the X Congresso Brasileiro de Energia Solar, Natal, Brasil.

Stein, J.S., Hansen, C.W., Reno, M.J., 2012. The variability index: a new and novel metric for quantifying irradiance and PV output variability. World Renewable Energy Forum.

Wendel, M., Colle, S., Cardemil, J.M., Miller, F.M., 2013. Metodologia para simulação transiente de uma pequena central heliotérmica.

Zhu, W., Zhang, L., Yang, M., Wang, B., 2019. Solar power ramp event forewarning with limited historical observations. In: 2019 IEEE/IAS 55th Industrial and Commercial Power Systems Technical Conference (I&CPS), 1–8.